In-operando X-ray tomography study of lithiation induced delamination of Si based anodes for lithium-ion batteries

Farid Tariq[1*], Vladimir Yufit[1], David S. Eastwood[2,3], Yu Merla[4], Moshiel Biton[1], Billy Wu[1], Zhangwei Chen[1], Kathrin Freedman[5], Gregory Offer[4], Emanuel Peled[5], Peter D. Lee[2,3], Diana Golodnitsky[5] and Nigel Brandon[1]

1. *Department of Earth Science and Engineering, Imperial College London, SW7 2AZ, UK*
2. *School of Materials, University of Manchester, Oxford Road, Manchester, M13 9PL, UK*
3. *Research Complex at Harwell, Harwell Oxford, Didcot, Oxfordshire, OX11 OFA, UK*
4. *Department of Mechanical Engineering, Imperial College London,SW7 2AZ, UK*
5. *Research School of Chemistry, Tel Aviv University, 4300 Israel*

(*corresponding author e-mail: farid.tarid02@imperial.ac.uk)

Keywords: Lithium-ion, Tomography, Silicon Anode

Abstract

Silicon-Lithium based rechargeable batteries offer high gravimetric capacity. However cycle life and electrode microstructure failure mechanisms remain poorly understood. Here we present an x-ray tomography method to investigate in-operando lithiation induced stress cracking leading to the delamination of a composite Si based electrode. Simultaneous voltage measurements show increased cell resistance correlating with severe delamination and microstructural changes. 3D analysis revealed 44.1% loss of the initial electrode-current collector area after 1 hour of operation at 2.4mA/cm^2 and a 21.2% increase in new anode surface area. The work represents a new basis for future investigation of Si-Li anodes.

1.0 Introduction

Lithium-ion batteries provide the highest energy and power density amongst existing secondary batteries, and are often favoured in energy storage applications. However, many applications require energy and capacity beyond current battery technologies.

Silicon anodes are an attractive alternative to carbon based anodes due to their high specific capacity (4200 mAh/g corresponding to $Li_{22}Si_5$ versus only 372 mAh/g for LiC_6) (1, 2). Despite this advantage, silicon based anodes suffer from up to 400% volume expansion resulting in poor cycle performance due to the loss of electroactive material upon continuous solid electrolyte interphase (SEI) growth and isolated island formation (3). To alleviate these adverse phenomena nano-stuctured silicon is usually mixed/coated with carbon and polymer binders (4, 5). Depending on the preparation route, significant improvement in performance and cycle life can be achieved (6). For example double-walled Si-C nanotubes and yolk-shell Si-C nanoparticles have been proposed as the most successful designs to diminish the negative effects of silicon expansion/contraction on charge/discharge (7).

The performance of composite silicon anodes is a strong function of a micro/nanostructure; therefore it is important to understand the ageing and failure mechanisms at these structural length scales in three dimensions, which remain comparatively poorly understood. X-ray radiography and tomography provides direct non-destructive imaging of microstructural evolutionary changes at length scales appropriate to the study of Si and SnO based anodes (3, 8, 9). Here, for the first time known to the authors, the development and implementation of a Si based battery anode imaging method is presented that enables *in-operando* tracking and 3D imaging of electrode microstructure. It is possible to explore evolutionary processes and

quantify them at fine length scales, in real time, and furthermore to study induced failure mechanisms as they occur. The work provides a platform for future studies to explore the effects of key factors such as preparation routes, composition, charge/discharge conditions, etc. on composite silicon anodes.

2.0 Experimental

A customised Si-Li half-cell was assembled in an argon filled glove box (Fig.1a). A lithium metal anode and a silicon-carbon composite cathode were used. The copper current collector rod was machined into a conical tip on the silicon side for X-ray imaging purposes. The final cathode composition was 70 wt.% carbon-coated Si, 20 wt.% Shawinigan Black Carbon (Chevron Chemicals), and 10 wt.% sodium carboxymethyl cellulose (Sigma-Aldrich). The carbon-coated Si power was prepared via pyrolysis of 60 wt.% Si 30nm nanoparticles (Umicore), 10 wt.% 50nm MWCNT (Skyspring Nanomaterials) and 30 wt.% of sugar(10). The current collector was dipcoated into Si/C slurry and vacuum dried in a furnace. Ionic liquid made from 1M LiPF6 EC:DEC 1:1 v/v and 2 wt.% of VC electrolyte (Solvionic) was the electrolyte. The active materials were enclosed by a Kapton® polyimide tube and sealed air-tight using Torr seal® epoxy (Goodfellow). The Si based anode (0.1-0.2mg) provides an estimated 200–400μAh capacity. The final design was 6mm in diameter and 53mm in length.

The electrochemical cell was mounted in an X-ray Microtomography (XMT) system (Phoenix v|tome|x, GE, USA) for direct imaging/tomography operated at 70 kV. Electrical wires were attached to the cell to lithiate the silicon anode and current control was maintained through an Ivium VERTEX (Ivium, Eindhoven, Netherlands) potentiostat. A galvanostatic charge current of 100μA was applied to the cell for 1 hour whilst monitoring voltage and simultaneously imaging the battery anode using X-rays (Fig.1a). After 1 hour the electrode was partially

lithiated and delamination was observed; then the current was stopped, electrical connectors removed and an X-ray tomography scan performed by rotating the sample. The 3D structure of the electrode, electrolyte and current collector was reconstructed using 602 projections captured over a 360° range and a filtered back projection algorithm; producing a total volume of 8mm^3 at a final voxel size of 9.3µm. Segmentation was carried out manually using Avizo Fire (FEI, Bordeux, France) to separate features of interest on both radiographic and tomographic datasets.

2.1 Modeling

An analogous 2D finite element model of the electrode was setup using Abaqus CAE to simulate stress distributions in the anode through lithiation induced volume expansion. The model was run in standard FE solver mode, with the assumption that 100 µA for 3500s would lead to a calculated 63 % volume expansion, and the silicon anode was isotropic, linear and elastic. An elastic modulus of 100 GPa and Poisson's ratio of 0.26 were used (11, 12). Several simulations were run with the anode circular interface fixed at angles from 240°, 180°, 120° and 60° respectively. The remaining part of the anode was allowed to move away from the current collector on volume expansion to follow the observed direction and effect of delamination (Fig.2).

3.0 Results and Discussion

This study successfully demonstrates a novel methodology for capturing valuable information *in-operando* of silicon based anode failure mechanisms. Previous *in-situ* x-ray methods have focused mostly upon SnO particles (9, 13), but not silicon based anodes which present difficulties in acquisition and data analysis due to low x-ray attenuation. The cone-tip design

95 employed here ensured that the entire surface of the current collector was covered in a low
96 attenuation X-ray observable silicon anode layer. This provides large areas of the electrode
97 that can be imaged for detail, and therefore maximised the likelihood of capturing observed
98 failure mechanisms. The compact cell design also minimises the object-source distance,
99 improving the X-ray resolution.
100
101 The results show a clear difference between two regions of the silicon electrode. The
102 electrode region in contact with an argon bubble (white in Fig.1c and supplementary material)
103 showed neither lithiation nor delamination, whereas the region in contact with the electrolyte
104 upon lithiation lifted off and delaminated in a concave 'bow shape' away from the current
105 collector. The inert bubble was present from battery manufacture. However, from these
106 results it is evident that lithiation results in anode expansion, that causes severe delamination.
107 Upon volumetric expansion, stresses are generated which are accommodated through the
108 creation of new surfaces and this results in the bowing of the anode away from the current
109 collector (Fig.1c-Fig.2). Interestingly, in a few locations the anode maintains good adhesion
110 with the current collector allowing the anode to continue to function; however, *in-operando*
111 imaging also shows that, during lithiation, delamination eventually results in areas of crack
112 propagation through the electrode thickness that reach the electrolyte. This is evident through
113 the 3D reconstruction (Fig.1b) where it is possible to see delamination leading to regions
114 where cracks propagate from the electrode-current collector interface through to the surface
115 of the electrode. The local electrode-current collector adhesion would influence this
116 behaviour. Over an operational lifetime, coalescence of cracks would therefore result in loss
117 of active material and hence capacity loss. The 3D data also shows the presence of intrinsic
118 porosity within the silicon electrode, although this accounts for < 1 vol %, these pores are

ca.30-50 μm wide and may facilitate crack propagation, and will be investigated in future studies.

Radiograph images during lithiation, at 100μA (current density of 2.4 mA/cm^2) show the delamination of the silicon electrode from the copper current collector (Fig.1c-Fig.2a). The height of the delamination continues to increase with charging time, as does the width but at a reducing rate. From the measured voltage data a rapid decrease in the cell potential is observed, suggesting that the electrode-current collector contact resistance is increasing due to the volumetric expansion caused by lithiation. After 500s the potential of the cell slightly decreases until reaching 1500s. An increase in the available active surface area caused by delamination may be responsible for this. Though 3D data analysis the electrode-current collector contact area decreases as a result of delamination by 1.84 mm^2 from an original 4.17mm^2 which is equivalent to a 44.1% loss of contact area (Fig.1c). Concurrently, the interfacial area between the delamination induced void and silicon anode increases to 2.13 mm^2, which corresponds to 21.2% of the total silicon anode area following lithiation. Consequently, the ability to track this is significant for cells since this fresh surface would result in capacity degradation through the consumption of lithium in SEI layer formation.

From the imaging results it is clear that lithiation induces electrode delamination. Simulations reveal that regions of the electrode fixed in contact with the current collector experience greater stresses (Fig.2b). The peak stresses occur at the beginning of the delamination void-current collector interface for all simulated angular positions. These positions correspond to the delamination crack tip in the imaging experiments, and delamination would therefore facilitate reducing stresses at the electrode-current collector interface. The imaging data suggests electrode delamination is not linear with time and interestingly, the modeling shows

that peak stresses decrease with decreasing angular position. A decrease in peak stresses could result in lower delamination rates with time. The present simulation is over-constrained, since stress relaxation simulations are beyond the scope of present work. Once these are considered then lower predicted peak stresses would be expected; however current values are of the same order of magnitude as those in literature (12), and most importantly similar trends are still expected to occur.

4.0 Conclusions

Here we present an X-ray radiographic and tomographic imaging methodology to study *in-operando* degradation mechanisms in a Si anode based battery. The lithiation induced stress cracking was sequentially followed by electrode-current collector delamination which led to an increase in contact resistance of the cell. Simulation results suggest peak stresses occur at the delamination location between the current collector and electrode. Quantitative analysis shows that 44.1% of the initial electrode-current collector area was lost within just 1 hour of operation at 100μA (2.4mA/cm^2). The volume expansion caused by the lithiation of the silicon anode resulted in 21.2 % of fresh electrode area being revealed.

The ability to quantify in 3D, the detailed microstructural evolutionary changes in a Si based anode as it operates provides opportunities to understand sources of battery degradation and failure. Furthermore, the approach is not limited to Si based anodes but can be applied to other chemistries, and offers insights into evolutionary microstructural changes and observed battery performance/lifetime.

Acknowledgements

167 The authors would like to thank: EPSRC Structural evolution across multiple time and length
168 scales project (EP/I02249X/1), EPSRC Energy Storage for Low Carbon Grids project
169 (EP/K002252/1), the US Office of Naval Research, the Materials for Aging Resistant Li-ion
170 High Energy Storage for Electric Vehicle Project, the Diamond-Manchester Collaboration and
171 the Research Complex at Harwell, Climate KIC, G.Cui and S.J.Cooper for assistance.

References

1. **H. Jung, *J Power Sources*, 115, 346 (2003).**

2. **K. Tokumitsu, H. Fujimoto, A. Mabuchi and T. Kasuh, 37, 1599 (1999).**

3. **U. Kasavajjula, C. Wang and a. J. Appleby, *J Power Sources*, 163, 1003 (2007).**

4. **Y. Liu, K. Hanai, J. Yang, N. Imanishi, A. Hirano and Y. Takeda, *Electrochemical and Solid-State Letters*, 7, A369 (2004).**

5. **N. S. Hochgatterer, M. R. Schweiger, S. Koller, P. R. Raimann, T. Wöhrle, C. Wurm and M. Winter, *Electrochemical and Solid-State Letters*, 11, A76 (2008).**

6. **M. L. Terranova, S. Orlanducci, E. Tamburri, V. Guglielmotti and M. Rossi, *J Power Sources*, 246, 167 (2014).**

7. **H. Wu and Y. Cui, *Nano Today*, 7, 414 (2012).**

8. **J. Wang, Y.-c. K. Chen-Wiegart and J. Wang, *Angewandte Chemie International Edition*, 53, 4460 (2014).**

9. **S.-C. Chao, Y.-C. Yen, Y.-F. Song, H.-S. Sheu, H.-C. Wu and N.-L. Wu, *J Electrochem Soc*, 158, A1335 (2011).**

10. **D. Golodnitsky, Advanced Silicon-Based Anodes for HighEnergy-Density Li-Ion Batteries, in, 3rd Israeli Power Sources Conference Tel-Aviv (2013).**

11. **V. A. Sethuraman, M. J. Chon, M. Shimshak, N. Van Winkle and P. R. Guduru, *Electrochem Commun*, 12, 1614 (2010).**

12. **G. Bucci, S. P. V. Nadimpalli, V. A. Sethuraman, A. F. Bower and P. R. Guduru, *Journal of the Mechanics and Physics of Solids*, 62, 276 (2014).**

13. **M. Ebner, F. Marone, M. Stampanoni and V. Wood, *Science*, 342, 716 (2013).**

Figure 1. a) Si based anode tomography cell construction and X-ray direction, b) 3D reconstruction after lithiation with delamination and, c) radiography during lithiation and delamination with voltage response.

Figure 2. a) Radiography based anode delamination and, b) 2D simulation of anode expansion with varying fixed boundary positions showing decreasing peak stresses with decreasing contact angle corresponding to increased delamination.

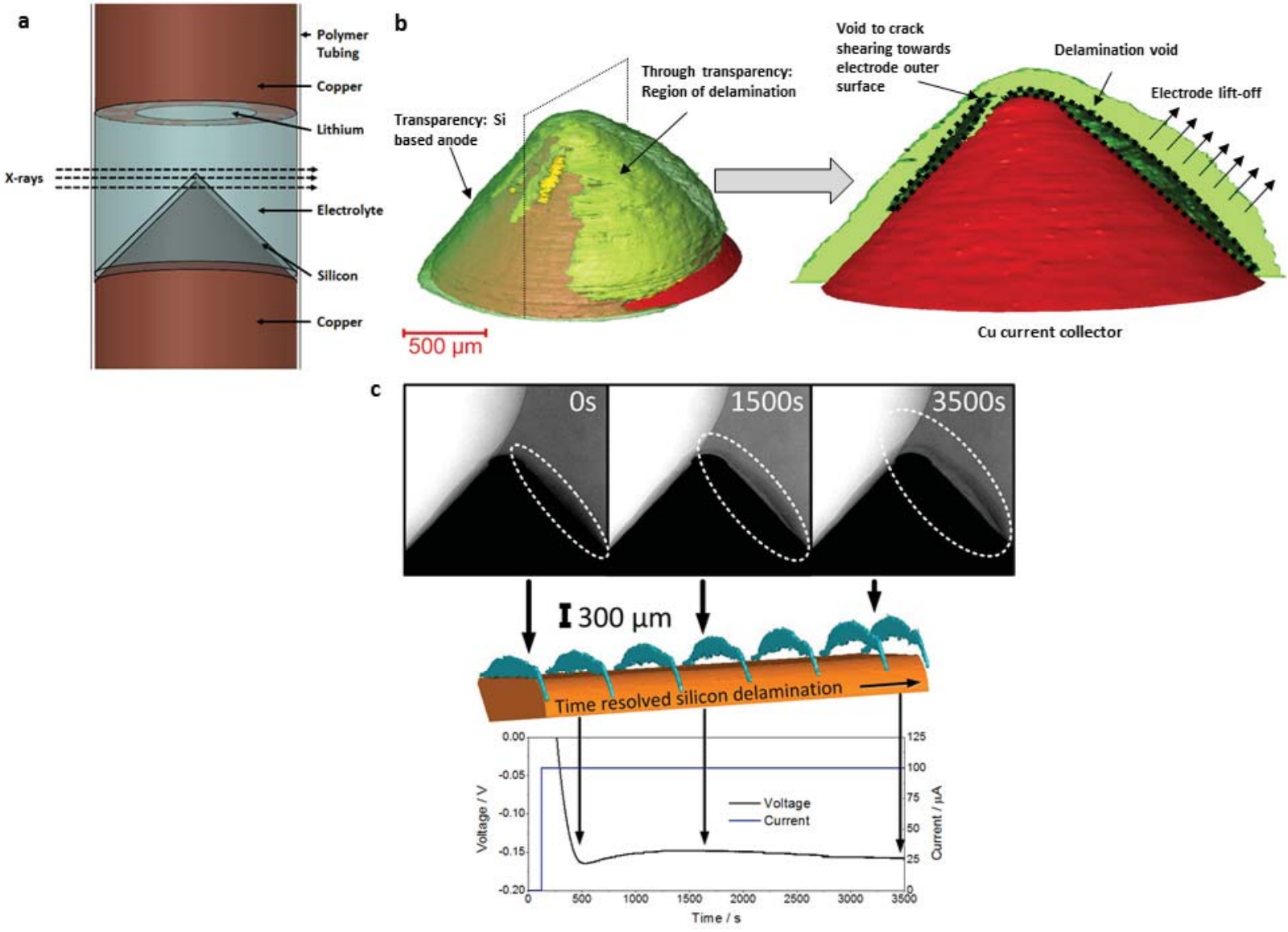
a
Polymer Tubing
Copper
Lithium
X-rays
Electrolyte
Silicon
Copper
b
Transparency: Si based anode
Through transparency: Region of delamination
Void to crack shearing towards electrode outer surface
Delamination void
Electrode lift-off
500 µm
Cu current collector
c
0s
1500s
3500s
300 µm
Time resolved silicon delamination
Voltage / V
Current / µA
Time / s
Voltage
Current

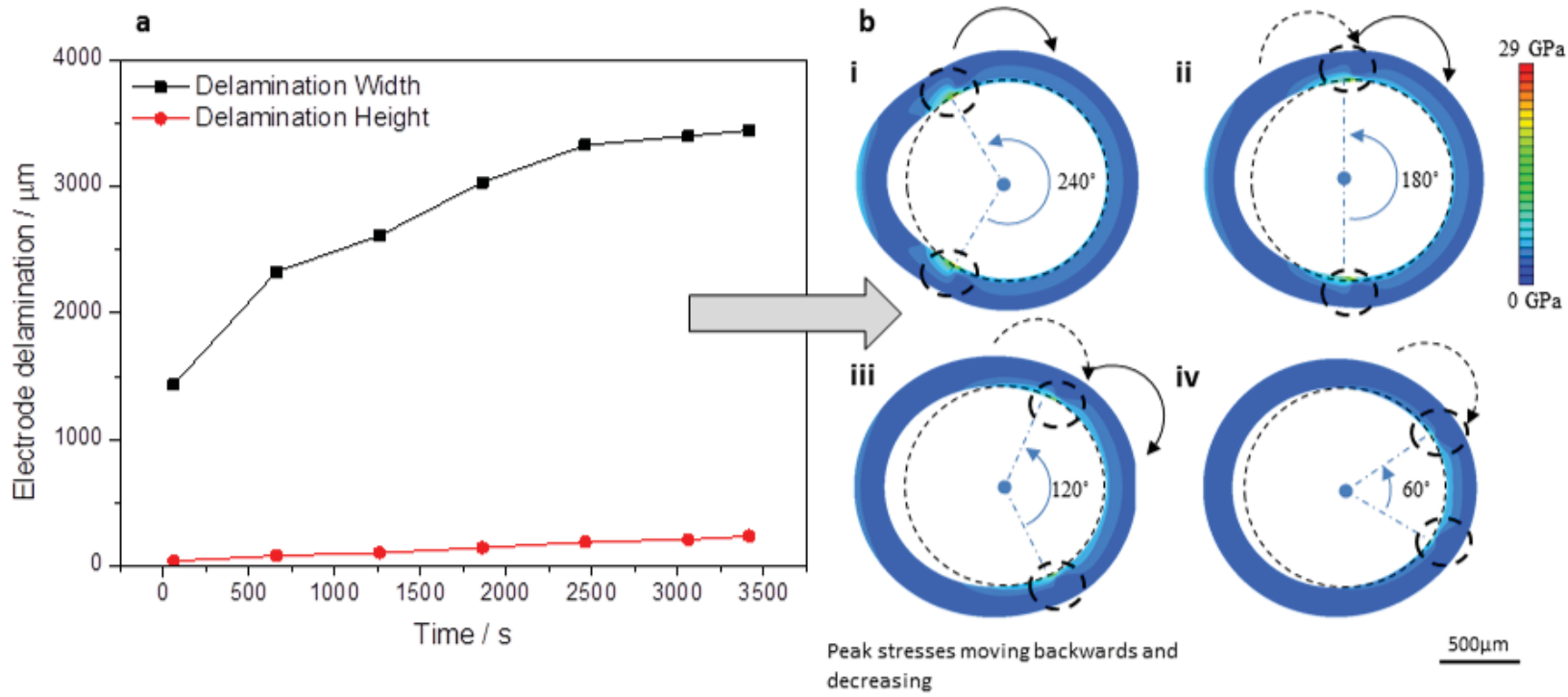
a
b
Delamination Width
Delamination Height
Electrode delamination / µm
Time / s
0
1000
2000
3000
4000
500
1500
2500
3500
i
ii
iii
iv
240°
180°
120°
60°
29 GPa
0 GPa
Peak stresses moving backwards and decreasing
500µm